The Astrophysical Journal, 681:1419–1430, 2008 July 10

IMPLICATIONS FOR THE ORIGIN OF GRB 070201 FROM LIGO OBSERVATIONS

B. Abbott,[1] R. Abbott,[1] R. Adhikari,[1] J. Agresti,[1] P. Ajith,[2] B. Allen,[2,3] R. Amin,[4] S. B. Anderson,[1] W. G. Anderson,[3] M. Arain,[5] M. Araya,[1] H. Armandula,[1] M. Ashley,[6] S. Aston,[7] P. Aufmuth,[8] C. Aulbert,[9] S. Babak,[9] S. Ballmer,[1] H. Bantilan,[10] B. C. Barish,[1] C. Barker,[11] D. Barker,[11] B. Barr,[12] P. Barriga,[13] M. A. Barton,[12] K. Bayer,[14] J. Betzwieser,[14] P. T. Beyersdorf,[15] B. Bhawal,[1] I. A. Bilenko,[16] G. Billingsley,[1] R. Biswas,[3] E. Black,[1] K. Blackburn,[1] L. Blackburn,[14] D. Blair,[13] B. Bland,[11] J. Bogenstahl,[12] L. Bogue,[17] R. Bork,[1] V. Boschi,[1] S. Bose,[18] P. R. Brady,[3] V. B. Braginsky,[16] J. E. Brau,[19] M. Brinkmann,[2] A. Brooks,[20] D. A. Brown,[1,21] A. Bullington,[22] A. Bunkowski,[2] A. Buonanno,[23] O. Burmeister,[2] D. Busby,[1] R. L. Byer,[22] L. Cadonati,[14] G. Cagnoli,[12] J. B. Camp,[24] J. Cannizzo,[24] K. Cannon,[3] C. A. Cantley,[12] J. Cao,[14] L. Cardenas,[1] G. Castaldi,[25] C. Cepeda,[1] E. Chalkley,[12] P. Charlton,[26] S. Chatterji,[1] S. Chelkowski,[2] Y. Chen,[9] F. Chiadini,[27] N. Christensen,[10] J. Clark,[12] P. Cochrane,[2] T. Cokelaer,[28] R. Coldwell,[5] R. Conte,[27] D. Cook,[11] T. Corbitt,[14] D. Coyne,[1] J. D. E. Creighton,[3] R. P. Croce,[25] D. R. M. Crooks,[12] A. M. Cruise,[7] A. Cumming,[12] J. Dalrymple,[29] E. D'Ambrosio,[1] K. Danzmann,[2,8] G. Davies,[28] D. DeBra,[22] J. Degallaix,[13] M. Degree,[22] T. Demma,[25] V. Dergachev,[30] S. Desai,[31] R. DeSalvo,[1] S. Dhurandhar,[32] M. Díaz,[33] J. Dickson,[6] A. Di Credico,[29] G. Diederichs,[8] A. Dietz,[28] E. E. Doomes,[34] R. W. P. Drever,[35] J.-C. Dumas,[13] R. J. Dupuis,[1] J. G. Dwyer,[36] P. Ehrens,[1] E. Espinoza,[1] T. Etzel,[1] M. Evans,[1] T. Evans,[17] S. Fairhurst,[1,28] Y. Fan,[13] D. Fazi,[1] M. M. Fejer,[22] L. S. Finn,[31] V. Fiumara,[27] N. Fotopoulos,[3] A. Franzen,[8] K. Y. Franzen,[5] A. Freise,[7] R. Frey,[19] T. Fricke,[37] P. Fritschel,[14] V. V. Frolov,[17] M. Fyffe,[17] V. Galdi,[25] J. Garofoli,[11] I. Gholami,[9] J. A. Giaime,[4,17] S. Giampanis,[37] K. D. Giardina,[17] K. Goda,[14] E. Goetz,[30] L. M. Goggin,[1] G. González,[4] S. Gossler,[6] A. Grant,[12] S. Gras,[13] C. Gray,[11] M. Gray,[6] J. Greenhalgh,[38] A. M. Gretarsson,[39] R. Grosso,[33] H. Grote,[2] S. Grunewald,[9] M. Guenther,[11] R. Gustafson,[30] B. Hage,[8] D. Hammer,[3] C. Hanna,[4] J. Hanson,[17] J. Harms,[2] G. Harry,[14] E. Harstad,[19] T. Hayler,[38] J. Heefner,[1] I. S. Heng,[12] A. Heptonstall,[12] M. Heurs,[2] M. Hewitson,[2] S. Hild,[8] E. Hirose,[29] D. Hoak,[17] D. Hosken,[20] J. Hough,[12] D. Hoyland,[7]

[1] LIGO California Institute of Technology, Pasadena, CA 91125.
[2] Albert-Einstein-Institut, Max-Planck-Institut für Gravitationsphysik, D-30167 Hannover, Germany.
[3] University of Wisconsin, Milwaukee, WI 53201.
[4] Louisiana State University, Baton Rouge, LA 70803.
[5] University of Florida, Gainesville, FL 32611.
[6] Australian National University, Canberra, ACT 0200, Australia.
[7] University of Birmingham, Birmingham B15 2TT, UK.
[8] Universität Hannover, D-30167 Hannover, Germany.
[9] Albert-Einstein-Institut, Max-Planck-Institut für Gravitationsphysik, D-14476 Golm, Germany.
[10] Carleton College, Northfield, MN 55057.
[11] LIGO Hanford Observatory, Richland, WA 99352.
[12] University of Glasgow, Glasgow G12 8QQ, UK.
[13] University of Western Australia, Crawley, WA 6009, Australia.
[14] LIGO Massachusetts Institute of Technology, Cambridge, MA 02139.
[15] San Jose State University, San Jose, CA 95192.
[16] Moscow State University, Moscow 119992, Russia.
[17] LIGO Livingston Observatory, Livingston, LA 70754.
[18] Washington State University, Pullman, WA 99164.
[19] University of Oregon, Eugene, OR 97403.
[20] University of Adelaide, Adelaide, SA 5005, Australia.
[21] California Institute of Technology–CaRT, Pasadena, CA 91125.
[22] Stanford University, Stanford, CA 94305.
[23] University of Maryland, College Park, MD 20742.
[24] NASA/Goddard Space Flight Center, Greenbelt, MD 20771.
[25] University of Sannio at Benevento, I-82100 Benevento, Italy.
[26] Charles Sturt University, Wagga Wagga, NSW 2678, Australia.
[27] University of Salerno, 84084 Fisciano (Salerno), Italy.
[28] Cardiff University, Cardiff CF24 3AA, UK.
[29] Syracuse University, Syracuse, NY 13244.
[30] University of Michigan, Ann Arbor, MI 48109.
[31] Pennsylvania State University, University Park, PA 16802.
[32] Inter-University Centre for Astronomy and Astrophysics, Pune 411007, India.
[33] University of Texas at Brownsville and Texas Southmost College, Brownsville, TX 78520.
[34] Southern University and A&M College, Baton Rouge, LA 70813.
[35] California Institute of Technology, Pasadena, CA 91125.
[36] Columbia University, New York, NY 10027.
[37] University of Rochester, Rochester, NY 14627.
[38] Rutherford Appleton Laboratory, Chilton, Didcot, Oxon OX11 0QX, UK.
[39] Embry-Riddle Aeronautical University, Prescott, AZ 86301.

S. H. Huttner,[12] D. Ingram,[11] E. Innerhofer,[14] M. Ito,[19] Y. Itoh,[3] A. Ivanov,[1] B. Johnson,[11] W. W. Johnson,[4] D. I. Jones,[40] G. Jones,[28] R. Jones,[12] L. Ju,[13] P. Kalmus,[36] V. Kalogera,[41] D. Kasprzyk,[7] E. Katsavounidis,[14] K. Kawabe,[11] S. Kawamura,[42] F. Kawazoe,[42] W. Kells,[1] D. G. Keppel,[1] F. Ya. Khalili,[16] C. Kim,[41] P. King,[1] J. S. Kissel,[4] S. Klimenko,[5] K. Kokeyama,[42] V. Kondrashov,[1] R. K. Kopparapu,[31] D. Kozak,[1] B. Krishnan,[9] P. Kwee,[8] P. K. Lam,[6] M. Landry,[11] B. Lantz,[22] A. Lazzarini,[1] M. Lei,[1] J. Leiner,[18] V. Leonhardt,[42] I. Leonor,[19] K. Libbrecht,[1] P. Lindquist,[1] N. A. Lockerbie,[43] M. Longo,[27] M. Lormand,[17] M. Lubinski,[11] H. Lück,[2,8] B. Machenschalk,[9] M. MacInnis,[14] M. Mageswaran,[1] K. Mailand,[1] M. Malec,[8] V. Mandic,[1] S. Marano,[27] S. Márka,[36] J. Markowitz,[14] E. Maros,[1] I. Martin,[12] J. N. Marx,[1] K. Mason,[14] L. Matone,[36] V. Matta,[27] N. Mavalvala,[14] R. McCarthy,[11] D. E. McClelland,[6] S. C. McGuire,[34] M. McHugh,[44] K. McKenzie,[6] S. McWilliams,[24] T. Meier,[8] A. Melissinos,[37] G. Mendell,[11] R. A. Mercer,[5] S. Meshkov,[1] C. J. Messenger,[12] D. Meyers,[1] E. Mikhailov,[14] S. Mitra,[32] V. P. Mitrofanov,[16] G. Mitselmakher,[5] R. Mittleman,[14] O. Miyakawa,[1] S. Mohanty,[33] G. Moreno,[11] K. Mossavi,[2] C. MowLowry,[6] A. Moylan,[6] D. Mudge,[20] G. Mueller,[5] S. Mukherjee,[33] H. Müller-Ebhardt,[2] J. Munch,[20] P. Murray,[12] E. Myers,[11] J. Myers,[11] T. Nash,[1] G. Newton,[12] A. Nishizawa,[42] K. Numata,[24] B. O'Reilly,[17] R. O'Shaughnessy,[41] D. J. Ottaway,[14] H. Overmier,[17] B. J. Owen,[31] Y. Pan,[23] M. A. Papa,[3,9] V. Parameshwaraiah,[11] P. Patel,[1] M. Pedraza,[1] S. Penn,[45] V. Pierro,[25] I. M. Pinto,[25] M. Pitkin,[12] H. Pletsch,[2] M. V. Plissi,[12] F. Postiglione,[27] R. Prix,[9] V. Quetschke,[5] F. Raab,[11] D. Rabeling,[6] H. Radkins,[11] R. Rahkola,[19] N. Rainer,[2] M. Rakhmanov,[31] M. Ramsunder,[31] S. Ray-Majumder,[3] V. Re,[7] H. Rehbein,[2] S. Reid,[12] D. H. Reitze,[5] L. Ribichini,[2] R. Riesen,[17] K. Riles,[30] B. Rivera,[11] N. A. Robertson,[1,12] C. Robinson,[28] E. L. Robinson,[7] S. Roddy,[17] A. Rodriguez,[4] A. M. Rogan,[18] J. Rollins,[36] J. D. Romano,[28] J. Romie,[17] R. Route,[22] S. Rowan,[12] A. Rüdiger,[2] L. Ruet,[14] P. Russell,[1] K. Ryan,[11] S. Sakata,[42] M. Samidi,[1] L. Sancho de la Jordana,[46] V. Sandberg,[11] V. Sannibale,[1] S. Saraf,[47] P. Sarin,[14] B. S. Sathyaprakash,[28] S. Sato,[42] P. R. Saulson,[29] R. Savage,[11] P. Savov,[21] S. Schediwy,[13] R. Schilling,[2] R. Schnabel,[2] R. Schofield,[19] B. F. Schutz,[9,28] P. Schwinberg,[11] S. M. Scott,[6] A. C. Searle,[6] B. Sears,[1] F. Seifert,[2] D. Sellers,[17] A. S. Sengupta,[28] P. Shawhan,[23] D. H. Shoemaker,[14] A. Sibley,[17] X. Siemens,[1,21] D. Sigg,[11] S. Sinha,[22] A. M. Sintes,[9,46] B. J. J. Slagmolen,[6] J. Slutsky,[4] J. R. Smith,[2] M. R. Smith,[1] K. Somiya,[2,9] K. A. Strain,[12] D. M. Strom,[19] A. Stuver,[31] T. Z. Summerscales,[48] K.-X. Sun,[22] M. Sung,[4] P. J. Sutton,[1] H. Takahashi,[9] D. B. Tanner,[5] R. Taylor,[1] R. Taylor,[12] J. Thacker,[17] K. A. Thorne,[31] K. S. Thorne,[21] A. Thüring,[8] K. V. Tokmakov,[12] C. Torres,[33] C. Torrie,[12] G. Traylor,[17] M. Trias,[46] W. Tyler,[1] D. Ugolini,[49] K. Urbanek,[22] H. Vahlbruch,[8] M. Vallisneri,[21] C. Van Den Broeck,[28] M. Varvella,[1] S. Vass,[1] A. Vecchio,[7] J. Veitch,[12] P. Veitch,[20] A. Villar,[1] C. Vorvick,[11] S. P. Vyachanin,[16] S. J. Waldman,[1] L. Wallace,[1] H. Ward,[12] R. Ward,[1] K. Watts,[17] A. Weidner,[2] M. Weinert,[2] A. Weinstein,[1] R. Weiss,[14] S. Wen,[4] K. Wette,[6] J. T. Whelan,[9] S. E. Whitcomb,[1] B. F. Whiting,[5] C. Wilkinson,[11] P. A. Willems,[1] L. Williams,[5] B. Willke,[2,8] I. Wilmut,[38] W. Winkler,[2] C. C. Wipf,[14] S. Wise,[5] A. G. Wiseman,[3] G. Woan,[12] D. Woods,[3] R. Wooley,[17] J. Worden,[11] W. Wu,[5] I. Yakushin,[17] H. Yamamoto,[1] Z. Yan,[13] S. Yoshida,[50] N. Yunes,[31] M. Zanolin,[14] J. Zhang,[30] L. Zhang,[1] C. Zhao,[13] N. Zotov,[51] M. Zucker,[14] H. zur Mühlen,[8] and J. Zweizig[1] (The LIGO Scientific Collaboration)[52]

and

K. C. Hurley[53]

Received 2007 December 1; accepted 2008 January 6

ABSTRACT

We analyzed the available LIGO data coincident with GRB 070201, a short-duration, hard-spectrum γ-ray burst (GRB) whose electromagnetically determined sky position is coincident with the spiral arms of the Andromeda galaxy (M31). Possible progenitors of such short, hard GRBs include mergers of neutron stars or a neutron star and a

[40] University of Southampton, Southampton SO17 1BJ, UK.
[41] Northwestern University, Evanston, IL 60208.
[42] National Astronomical Observatory of Japan, Tokyo 181-8588, Japan.
[43] University of Strathclyde, Glasgow G1 1XQ, UK.
[44] Loyola University, New Orleans, LA 70118.
[45] Hobart and William Smith Colleges, Geneva, NY 14456.
[46] Universitat de les Illes Balears, E-07122 Palma de Mallorca, Spain.
[47] Rochester Institute of Technology, Rochester, NY 14623.
[48] Andrews University, Berrien Springs, MI 49104.
[49] Trinity University, San Antonio, TX 78212.
[50] Southeastern Louisiana University, Hammond, LA 70402.
[51] Louisiana Tech University, Ruston, LA 71272.
[52] See http://www.ligo.org.
[53] University of California, Berkeley, Space Sciences Lab, 7 Gauss Way, Berkeley, CA 94720.

black hole, or soft γ-ray repeater (SGR) flares. These events can be accompanied by gravitational-wave emission. No plausible gravitational-wave candidates were found within a 180 s long window around the time of GRB 070201. This result implies that a compact binary progenitor of GRB 070201, with masses in the range $1\ M_\odot < m_1 < 3\ M_\odot$ and $1\ M_\odot < m_2 < 40\ M_\odot$, located in M31 is excluded at >99% confidence. If the GRB 070201 progenitor was not in M31, then we can exclude a binary neutron star merger progenitor with distance $D < 3.5$ Mpc, assuming random inclination, at 90% confidence. The result also implies that an unmodeled gravitational-wave burst from GRB 070201 most probably emitted less than $4.4 \times 10^{-4}\ M_\odot c^2$ (7.9×10^{50} ergs) in any 100 ms long period within the signal region if the source was in M31 and radiated isotropically at the same frequency as LIGO's peak sensitivity ($f \approx 150$ Hz). This upper limit does not exclude current models of SGRs at the M31 distance.

Subject headings: gamma rays: bursts — gravitational waves — methods: data analysis

Online material: color figures

1. INTRODUCTION

Gamma-ray bursts (GRBs) are intense flashes of γ-rays which are observed to be isotropically distributed over the sky (see, e.g., Klebesadel et al. 1973; Piran 2005; Mészáros 2002 and references therein). The variability of the bursts on short timescales indicates that the sources are very compact. Combined observations, using γ-ray and X-ray satellites such as *Vela*,[54] *CGRO*,[55] *BeppoSax*,[56] *HETE*,[57] *Swift*,[58] Konus-*Wind*,[59] and the *INTEGRAL*[60] missions (see Klebesadel et al. 1973; Meegan et al. 1992; Paciesas et al. 1999; Frontera et al. 2000; Mazets & Golenetskii 1981; Gehrels et al. 2004 and references therein), as well as by the Interplanetary Network (IPN), with follow-up by X-ray, optical, and radio telescopes of the region around GRBs, have yielded direct observations of afterglows from ≈350 GRBs. In turn, host galaxies were identified for many GRBs, and redshifts were determined for ≈125 bursts. The redshifts indicated that GRBs are of extragalactic origin. Two types of GRBs are distinguished by their characteristic duration (see Kouveliotou et al. 1993; Gehrels et al. 2006) and are understood to have different origins.

Long GRBs have durations $\gtrsim$2 s. Detailed observations of long GRBs demonstrate their association with star-forming galaxies ranging up to a redshift of $z \approx 6.3$ (see Kawai et al. 2006; Watson et al. 2006; Jakobsson et al. 2006 and references therein). Furthermore, several nearby long GRBs have been spatially and temporally coincident with supernovae (e.g., Campana et al. 2006; Malesani et al. 2004; Hjorth et al. 2003; Galama et al. 1998; Woosley & Bloom 2006).

Short GRBs have durations $\lesssim$2 s. The progenitors of short GRBs are not so well understood. While there are associations with distant galaxies of different types and different star formation histories, there are also powerful bursts of γ-rays from Galactic sources, such as SGR 1806−20 (Nakar et al. 2006; Hurley et al. 2005; Palmer et al. 2005). However, statistical analyses indicate that at most 15% of known short GRBs can be accounted for as soft γ-ray repeaters (SGRs; Nakar et al. 2006; Chapman et al. 2008). Moreover, the spectral characteristics and energetics of some observed short GRBs and their afterglows seem to contradict this hypothesis in most cases (Nakar et al. 2006). The current leading hypothesis to explain most short GRBs is the merger of neutron stars or neutron star + black hole binaries (see, e.g., Nakar 2007; Bloom et al. 2007 and references therein). However, to date no observations have definitively confirmed the association between short GRBs and binary mergers.

Therefore, given the candidate sources, it is plausible that GRB central engines are also strong gravitational-wave (GW) emitters at frequencies accessible to ground-based detectors like the Laser Interferometer Gravitational-wave Observatory (LIGO), GEO-600, and Virgo (Abbott et al. 2005a, 2005b, 2006a; Acernese et al. 2006; Willke et al. 2002; Kochanek & Piran 1993; Finn et al. 2004). Bursts of gravitational waves are expected to be emitted during the GRB event, with a characteristic duration comparable to that of the associated GRB, although the amplitude and frequency spectra of the gravitational-wave burst are unknown. In the case of short GRBs produced by compact binary mergers, gravitational waves with relatively well-modeled amplitude and frequency evolution will be emitted during the inspiral phase of the binary system, preceding the event that produces the GRB.

GRB 070201 was an intense, short-duration, hard-spectrum GRB which was detected and localized by three IPN spacecraft (Konus-*Wind*, *INTEGRAL*, and *MESSENGER*); it was also observed by *Swift* (BAT), but with a high-intensity background, as the satellite was entering the South Atlantic Anomaly (Golenetskii et al. 2007b). The burst light curve exhibited a multipeaked pulse with a duration of ∼0.15 s, followed by a much weaker, softer pulse that lasted ∼0.08 s. Using early reports, Perley & Bloom (2007) pointed out that the initial IPN location annulus of the event intersected the outer spiral arms of the Andromeda galaxy (M31). The refined error box, centered $\approx 1.1^\circ$ from the center of M31, was later reported (Pal'shin 2007; Hurley et al. 2007), and it still overlaps the spiral arms of M31 (see Fig. 1; E. Mazets et al. 2007, private communication; Mazets et al. 2008).[61] Based on the Konus-*Wind* observations (Mazets et al. 2008; Golenetskii et al. 2007a), the burst had a fluence of $1.57^{-0.21}_{+0.06} \times 10^{-5}$ ergs cm^{-2} in the 20 keV−1 MeV range.

It was also pointed out (Golenetskii et al. 2007a) that if the burst source were actually located in M31 (at a distance of ≃770 kpc) the isotropic energy release would be $\sim 10^{45}$ ergs, comparable to the energy release in giant flares of soft SGRs, e.g., the 1979 March 5 event from SGR 0526−66 ($\sim 2 \times 10^{44}$ ergs in the initial pulse) and the 2004 December 27 event from SGR 1806−20 ($\sim 2 \times 10^{46}$ ergs). Conversely, if the event had an isotropic energy release more typical of short, hard GRBs, e.g., $\sim 10^{48}$–10^{52} ergs (Berger 2007), then it would have to be located at least ∼30 times further than M31 (i.e., further than ∼23 Mpc).

At the time of GRB 070201, the Hanford detectors of LIGO (Abbott et al. 2004) were stable and recording science-quality data, while the LIGO Livingston, GEO-600, and Virgo detectors were not taking data. The LIGO data around GRB 070201 were

[54] See http://heasarc.gsfc.nasa.gov/docs/heasarc/missions/vela5a.html.
[55] See http://www.batse.msfc.nasa.gov/batse/.
[56] See http://bepposax.gsfc.nasa.gov/bepposax/index.html.
[57] See http://space.mit.edu/HETE/.
[58] See http://www.swift.psu.edu/.
[59] See http://heasarc.gsfc.nasa.gov/docs/heasarc/missions/wind.html.
[60] See http://www.esa.int/SPECIALS/Integral/SEME2V0XDYD_0.html.
[61] See also http://www.ssl.berkeley.edu/ipn3/.

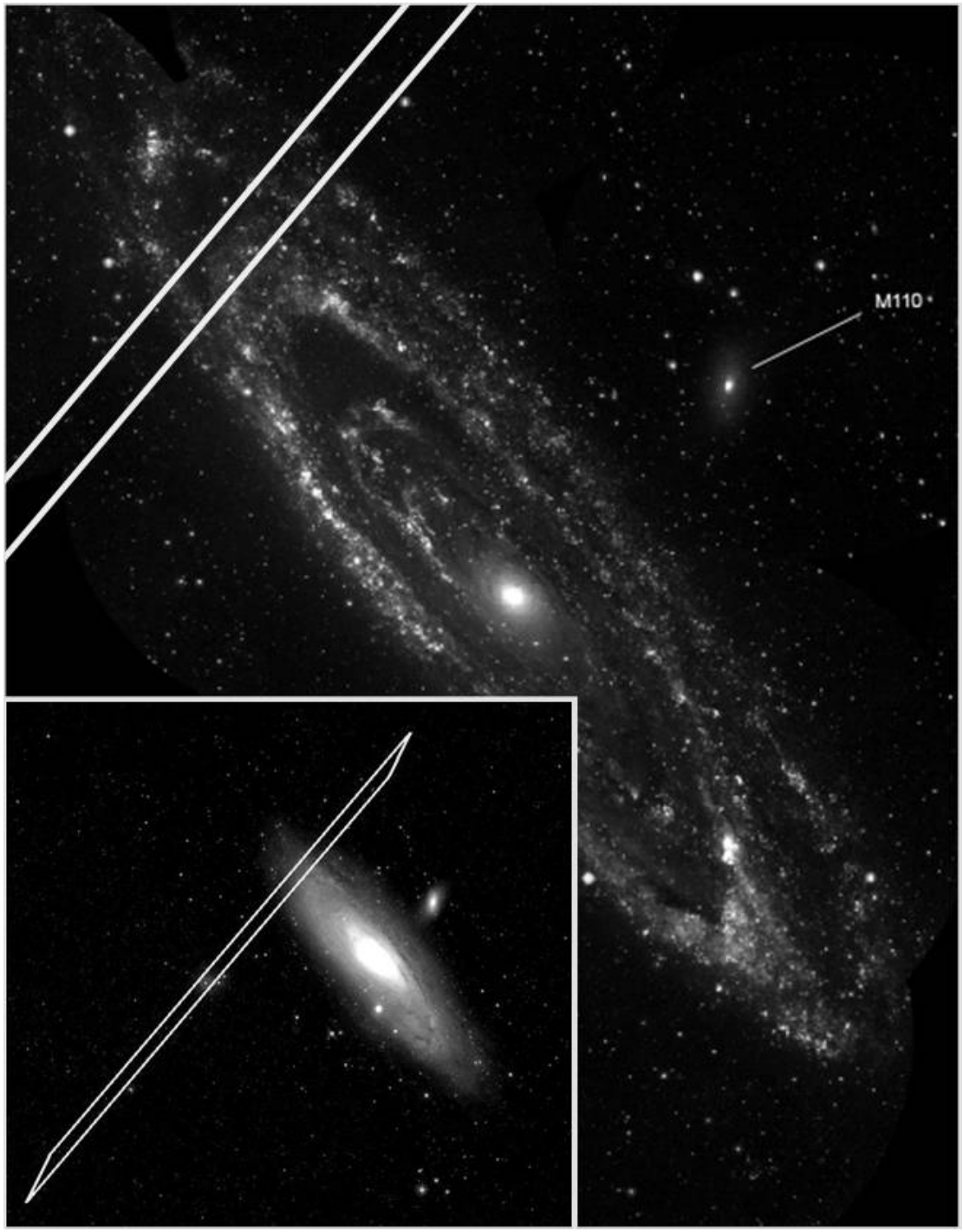

FIG. 1.—IPN3 (γ-ray) error box overlapping the spiral arms of the Andromeda galaxy (M31). The inset image shows the full error box superimposed on an SDSS (Adelman-McCarthy et al. 2006; SDSS, http://www.sdss.org/) image of M31. The main panel shows the overlap of the error box and the spiral arms of M31 in UV light (Thilker et al. 2005). [*See the electronic edition of the Journal for a color version of this figure.*]

searched for evidence of a gravitational-wave signal from the compact binary inspiral or the central engine of the GRB itself.

A standard measure of the sensitivity of a detector to gravitational waves is the distance to which an optimally oriented and located double neutron star binary would produce a response in the data stream that, when optimally filtered for the inspiral waves, peaks at a signal-to-noise ratio (S/N) of 8 (see, e.g., Abbott et al. 2005b and references therein). At the time of GRB 070201, this distance was 35.7 and 15.3 Mpc for the Hanford 4 and 2 km detectors, respectively. However, the sensitivity of a detector to a gravitational wave depends on the location of the source on the sky and on the polarization angle of the waves. In the case of compact binaries, it also depends on the inclination angle of the orbital plane relative to the line of sight. At the time of GRB 070201, the binary inspiral reach in the direction of M31 was only about 43% of this maximum. More details of the instrumental sensitivity can be found in § 2.

The search for gravitational waves from a compact binary inspiral focused on objects with masses in the ranges $1\ M_\odot < m_1 < 3\ M_\odot$ and $1\ M_\odot < m_2 < 40\ M_\odot$. The core of the search is matched

filtering, cross-correlating the data with the expected gravitational-wave waveform for the binary inspiral, and uses methods reported previously (see, e.g., Abbott et al. 2005b and references therein). Uncertainties in the expected waveforms can lead to decreased sensitivity of the search to the gravitational-wave signal from the inspiral phase; this is particularly true of systems with higher masses and substantial spin (Grandclement et al. 2003). This is accounted for by studying the dependence of the sensitivity of the search to a variety of model waveforms based on different approximation methods.

The search for more generic transient gravitational waves coincident with the GRB is based on cross-correlating data from two detectors and does not make use of a specific model for the gravitational-wave signal. This is an appropriate method when the gravitational-wave signal is not well modeled theoretically, such as signals from the actual merger phase of a compact binary system or the core-collapse phase of a supernova event.

The remainder of the paper is organized as follows. In § 2 we discuss the LIGO detectors and the data taken around the time of GRB 070201. In § 3 we report on the inspiral gravitational-wave search, briefly reviewing the methods and algorithms used and concluding with the astrophysical implications of the search for the GRB 070201 event. In § 4 we report on the search for burst-like gravitational-wave signals and present the astrophysical implications of that search. The software used in this analysis is available in the LIGO Scientific Collaboration's data analysis code archives.[62] Since no plausible gravitational-wave signal was detected above the background in either the inspiral or the burst search, we present the astrophysical implications of these results on the understanding of short GRBs in § 5.

2. LIGO OBSERVATIONS

LIGO is comprised of three instruments at two geographically distinct locations (a 4 km detector and a 2 km detector at Hanford Observatory, referred to as H1 and H2, and a 4 km detector at Livingston Observatory, referred to as L1). Five science runs have been carried out to date. GRB 070201 occurred during the most recent science run, called S5, which started on 2005 November 4 and ended on 2007 October 1. All three LIGO detectors were operating at their design sensitivity[63] throughout the S5 run.

The LIGO detectors use suspended mirrors at the ends of kilometer-scale, orthogonal arms to form a power-recycled Michelson interferometer with Fabry-Pérot cavities. A gravitational wave induces a time-dependent strain $h(t)$ on the detector. While acquiring scientific data, feedback to the mirror positions and to the laser frequency keeps the optical cavities near resonance, so that interference in the light from the two arms recombining at the beam splitter depends on the difference between the lengths of the two arms. A photodiode senses the light, and a digitized signal is recorded at a sampling rate of 16,384 Hz. The data are calibrated and converted into a strain time series.

The LIGO detectors have a sensitive frequency band extending from $\sim$40 to $\sim$2000 Hz, with the maximum sensitivity at $\approx$150 Hz, which is limited at low frequencies by seismic noise and at high frequencies by laser shot noise. In addition, environmental disturbances, control systems noise, and other well-understood noise sources result in a nonstationary and non-Gaussian background.

[62] See http://www.lsc-group.phys.uwm.edu/cgi-bin/cvs/viewcvs.cgi/?cvsroot=lscsoft. The search for inspiraling binaries (§ 3) used LAL and LALAPPS with tag s5_grb070201_20070731, and the burst search (§ 4) used the MATAPPS package `grbxcorr` with tag grbxcorr_r1.

[63] See http://www.ligo.caltech.edu/docs/G/G060009-03/.

2.1. *LIGO Observations Coincident with GRB 070201*

At the time of the GRB trigger, both LIGO Hanford detectors were stable and recording science-quality data. These detectors had been in science mode for more than 14 hr before the GRB trigger, and they stayed in science mode for more than 8 hr after the GRB trigger, providing ample data for background studies.

An asymmetric 180 s *on-source* segment, −120/+60 s about the GRB trigger time, was searched for gravitational-wave signals. This choice (Abbott et al. 2005a, 2008a) was conservative enough to accommodate inspiral-type signals, trigger time ambiguities, and theoretical uncertainties. We also implicitly assumed that the propagation speed of the gravitational waves was the speed of light. The significance of candidate events was evaluated using studies covering several hours of *off-source* data from the same science mode stretch outside of, but near, the on-source segment.

The ideal response of a detector to an incident gravitational wave is a weighted combination of the two underlying gravitational-wave polarizations denoted by $h_+(t)$ and $h_\times(t)$,

$$h(t) = F_+(\theta, \phi, \psi)h_+(t) + F_\times(\theta, \phi, \psi)h_\times(t). \quad (1)$$

The dimensionless weighting amplitudes, or *antenna factors*, F_+ and $F_\times$, depend on the position (θ, ϕ) of the source relative to the detector and the gravitational-wave polarization angle ψ. For the location of GRB 070201, the rms antenna factor, $F_{\rm rms}$, for both colocated and coaligned Hanford detectors was

$$F_{\rm rms} = \sqrt{\left(F_+^2 + F_\times^2\right)/2} = 0.43/\sqrt{2} = 0.304, \quad (2)$$

a combination which does not depend on the polarization angle ψ. Despite the suboptimal location of GRB 070201 for the LIGO Hanford detectors, they still had significant sensitivity for the polarization state compatible with the detector.

2.2. *Data Quality for the Times Surrounding the GRB 070201 Trigger*

A suite of data quality tests were applied to the LIGO data. No anomalous behavior was found in either instrument at the time of GRB 070201. On the other hand, a number of data quality issues were identified in the off-source time used for background estimation (which amounted to 60,084 s, or 16.7 hr). Triggers were excluded from 530 s of coincident, off-source data so identified, or 0.9% of the off-source time.

Overflows in digital signals used in the feedback control systems were responsible for 29 s in H1 and 29 s in H2 of excluded time. Seismic noise in the 3–10 Hz band known to produce false alarms in H1 was used to veto 160 s of data. Disturbances that produced a loss in power in the H2 detector arm cavities larger than 4% were also vetoed, amounting to 163 s, which include 11 s when there were overflows in H2. No such fluctuations in arm power were observed in H1.

In addition, in the search for a compact binary progenitor, there were losses in off-source live time due to quantization on 180 s intervals. Each of these intervals was intended to be a trial treated the same as the central, on-source interval for use in background determination.

For the burst analysis, 3 hr of data were used for the purpose of background estimation. The same data quality flags were considered as were used in the inspiral search, but, due to the shorter length of the background used, only one data quality flag (an overflow in the H2 signal) was applied, vetoing one of the 180 s segments in the 3 hr background period.

Finally, 160 s of the off-source time were excluded from this data analysis, as it contained simulated signals. These were injected intentionally into the hardware at predetermined times to validate the detector response and signal detection algorithms.

3. SEARCH FOR GRAVITATIONAL WAVES FROM A COMPACT BINARY PROGENITOR

A number of searches for gravitational waves from compact binaries have been completed on the LIGO data (Abbott et al. 2005b, 2005c, 2006b, 2008b). Similar search methods were applied to the on-source time around GRB 070201 (Abbott et al. 2008b). In this section we briefly describe those methods, report the results of the search, and discuss their interpretation.

3.1. *Search Method*

The core of the inspiral search involves correlating the LIGO data against the theoretical waveforms expected from compact binary coalescence, i.e., matched-filtering the data (Wainstein & Zubakov 1962). The gravitational waves from the inspiral phase, when the binary orbit tightens under gravitational-wave emission prior to merger, are accurately modeled in the band of LIGO sensitivity for a wide range of binary masses (Blanchet 2006). The expected gravitational-wave signal, as measured by LIGO, depends on the masses and spins of the binary elements, as well as the spatial location, inclination, and orientation of the orbital axis. In general, the power of matched filtering depends most sensitively on accurately tracking the phase evolution of the signal. The phasing of compact binary inspiral signals depends on the masses and spins, the time of merger, and an overall phase. In a search for gravitational waves from compact binaries, one therefore uses a discrete set of *template waveforms* against which the data are correlated.

In this search, we adopt template waveforms which span a two-dimensional parameter space (one for each component mass) such that the maximum loss in S/N for a binary with negligible spins would be 3%. While the spin is ignored in the template waveforms, we show below that the search is still sensitive to the binaries with the most physically reasonable spin orientations and magnitudes with only moderate loss in sensitivity. To generate a GRB, at least one of the objects in a compact binary must be a material object, probably a neutron star, while the second object must be either a neutron star or a stellar mass black hole with low enough mass (Vallisneri 2000; Rantsiou et al. 2008) to cause disruption of the neutron star before it is swallowed by the hole. The mass-parameter space covered by the templates is therefore $1\ M_\odot < m_1 < 3\ M_\odot$ and $1\ M_\odot < m_2 < 40\ M_\odot$. The number of template waveforms required to achieve this coverage depends on the detector noise curve; at the time of the GRB, 7171 and 5417 templates were required in H1 and H2, respectively.

The data from each of the LIGO instruments are filtered through the bank of templates. If the matched filter S/N exceeds a threshold ρ^*, the template masses and the time of the maximum S/N are recorded. For a given template, threshold crossings are clustered using a sliding window equal to the duration of the template, as explained in Allen et al. (2005). For each trigger identified in this way, the coalescence phase and the effective distance—the distance at which an optimally oriented and located binary would give the observed S/N assuming masses to be those of the template—are also computed. Triggers identified in each instrument are further required to be coincident in the time and mass parameters between the two operating instruments, taking into account the correlations between those parameters. This significantly reduces the number of background triggers that arise from matched filtering in each instrument independently. Because H1 was more sensitive than H2, two different thresholds were used in the matched-filtering step: $\rho^* = 5.5$ in H1 and $\rho^* = 4.0$ in H2. This choice takes advantage of the better sensitivity in H1 while still using H2 to reduce the rate of accidentals.

To further reduce the background, two signal-based tests are applied to the data. First, a χ^2 statistic (Allen 2005), which measures the quality of the match between the data and the template, is computed; triggers with large χ^2 are discarded. Second, the r^2 veto (Rodriguez 2007), which looks at the time the χ^2 statistic stays above a threshold, is applied.

The S/N and χ^2 from a single detector are combined into an effective S/N (Abbott et al. 2008b). The effective S/Ns from the two detectors are then added in quadrature to form a single quantity, $\rho^2_{\rm eff}$, which provides good separation between signal candidate events and background. The final list of coincident triggers is then called the *candidate events*.

3.2. *Background and Results*

Gravitational-wave detectors are susceptible to many sources of environmental and intrinsic noise. These sources often result in non-Gaussian and nonstationary noise backgrounds. In the case of H1 and H2, which share the same vacuum enclosure, these backgrounds are correlated. To estimate the background in this search, an equal number of 180 s long off-source segments were selected from the past and from the future of the GRB trigger. All of the data, including the on-source segment, were analyzed using the methods described above. Triggers arising from the on-source segment were then removed, as were triggers within bad-quality segments, leading to an estimate of the number of accidental triggers per 180 s segment. A total off-source time of 56,340 s was analyzed, corresponding to 313 trials of 180 s. The mean rate of coincidence was 2.4 per 180 s segment.

Figure 2 shows the expected number of coincidences above each $\rho^2_{\rm eff}$ value in 180 s based on the analysis of the off-source times (Abbott et al. 2008b). No candidates were observed in the on-source time. Therefore, no plausible gravitational-wave signals from compact binary coalescence were identified around the time of GRB 070201.

3.3. *Astrophysical Interpretation*

The observations reported here can be used to constrain the distance to the GRB, assuming it was caused by a compact binary merger. With similar considerations, one can also evaluate the probability that a compact binary progenitor at the distance of M31 was responsible for GRB 070201.

We discover these bounds by computing the likelihood of our observation, namely, the probability that no signal would be observed in the on-source time, given the presence of a compact binary progenitor with various parameters. Denote the gravitational-wave signal by $h(t; m_2, D, \boldsymbol{\mu})$, where m_2 is the mass of the companion, D is the physical distance to the binary, and $\boldsymbol{\mu} = \{m_1, \boldsymbol{s}_1, \boldsymbol{s}_2, \iota, \Phi_0, t_0\}$ is the mass of the neutron star, the spins, the inclination, the coalescence phase, and the coalescence time. The probability of interest is then

$$p[0|h(t; m_2, D)] = \int p(\boldsymbol{\mu}) p[0|h(t; m_2, D, \boldsymbol{\mu})]\, d\boldsymbol{\mu}, \qquad (3)$$

where the nuisance parameters $\boldsymbol{\mu}$ are integrated over some prior distribution $p(\boldsymbol{\mu})$. This integration was performed by injecting simulated signals into the data streams of both detectors according to the desired prior distribution and evaluating the efficiency for recovering those injections as candidate events (as described

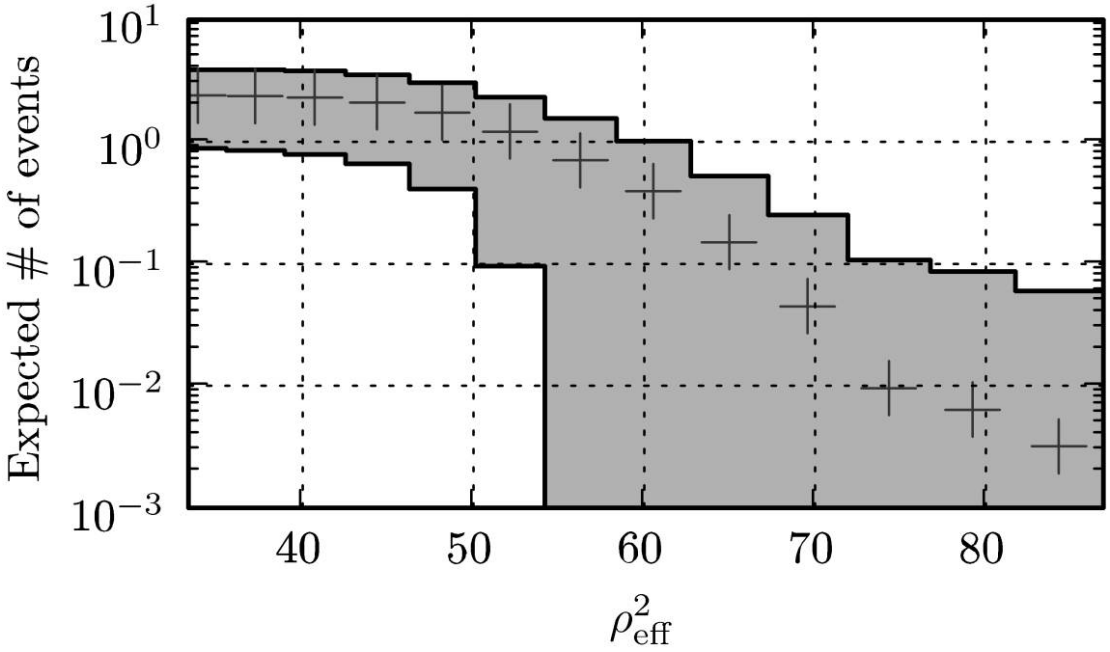

FIG. 2.—Cumulative histogram of the expected number of background triggers in 180 s based on the analysis of the off-source times (*plus signs*) as a function of the effective S/N (Abbott et al. 2008b). The shaded region indicates the 1 σ variation in the background estimate observed in the off-source times. [*See the electronic edition of the Journal for a color version of this figure.*]

in § 3.1) as a function of m_2 and D. We choose uniform priors over m_1 ($1\ M_\odot < m_1 < 3\ M_\odot$), Φ_0, t_0, and the polarization angle; the priors for spin and inclination ι are discussed below.

Astrophysical black holes are expected to have substantial spin. The maximum allowed by accretion spin-up of the hole is $(a/M) = (cS/GM^2) < 0.9982$ (Thorne 1974) in units of the Kerr spin parameter (S is the spin angular momentum of the black hole). More detailed simulations and recent observations provide a broad range of values (O'Shaughnessy et al. 2005) with a maximum observed spin $(a/M) > 0.98$ (McClintock et al. 2006). The maximum spin that a neutron star can have is estimated from a combination of simulations and observations of pulsar periods. Numerical simulations of rapidly spinning neutron stars give $(a/M) < 0.75$ (Cook et al. 1994); the maximal spin of the observed pulsar sample may be substantially lower than that. In our spinning simulations, we adopted a distribution in which the spin magnitudes are uniformly distributed between zero and $(a/M) = (cS/GM^2) = 0.98$ and $(a/M) = (cS/GM^2) = 0.75$ for the black holes and neutron stars, respectively, while the direction of each spin is uniform over the sphere. There is strong evidence that short GRBs are beamed (see, e.g., Soderberg et al. 2006; Nakar 2007; Burrows et al. 2006 and references therein), although probably less so than long bursts (Grupe et al. 2006). If this is the case, the most likely direction for beaming is along the total angular momentum vector of the system. For binaries with small component spins, this will correspond to the direction orthogonal to the plane of the orbit. Hence, the inclination angle of the binary, relative to the line of sight, is most likely to be close to zero. However, since zero inclination is the best case for detection of gravitational waves, a uniform prior on $\cos\iota$ provides a conservative constraint. We drew $\cos\iota$ from a uniform prior.

Figure 3 shows the contours of constant probability $1 - p[0|h(t; m_2, D)]$. Compact binaries corresponding to parameters (m_2, D) in the darkest shaded region are excluded as progenitors for this event at the 90% confidence level. As a reference point, a compact binary progenitor with masses $1\ M_\odot < m_1 < 3\ M_\odot$ and $1\ M_\odot < m_2 < 4\ M_\odot$ with $D < 3.5$ Mpc is excluded at 90% confidence; the same system with $D < 8.8$ Mpc is excluded at the 50% level. This result is averaged over different theoretical waveform families; 20% of the simulated waveforms include spins sampled as described above.

A number of systematic uncertainties enter into this analysis, but amplitude calibration error (≈10%) and Monte Carlo statistics have the largest effects. These uncertainties have been folded into our analysis in a manner similar to that described in Abbott et al. (2005b, 2005c). In particular, the amplitude calibration was taken into account by scaling the distance of the injection signal to be $1.28 \times 10\%$ larger; the Monte Carlo error adds $1.28[p(1-p)/n]^{1/2}$ to $p = p[0|h(t; m_2, D)]$, where n is the total number of simulated signals in a particular mass-distance bin.

We evaluate the hypothesis that the event occurred in M31, as electromagnetic observations hint might be the case, given our observation. We adopt the measured distance of 0.77 Mpc to M31. We then simulate a large number of inspirals at distances 0.77 Mpc $< D <$ 0.9 Mpc, which allows us to account for both uncertainty in distance to M31 (7%; Freedman et al. 2001) and the amplitude calibration uncertainty discussed above. The simulations exclude any compact binary progenitor in our simulation space at the distance of M31 at the >99% level.

4. SEARCH FOR A GRAVITATIONAL-WAVE BURST

To search for a gravitational-wave burst associated with GRB 070201 we have used LIGO's current baseline method for near–real time searches for gravitational-wave bursts associated with GRB triggers.[64] A detailed description of the analysis method is presented elsewhere (Abbott et al. 2008a).

4.1. *Search Method*

The burst search method is based on cross-correlating a pair of preconditioned data streams from two different gravitational-wave detectors. The preconditioning of the data streams consists

[64] See http://www.ssl.berkeley.edu/ipn3/ and http://gcn.gsfc.nasa.gov/.

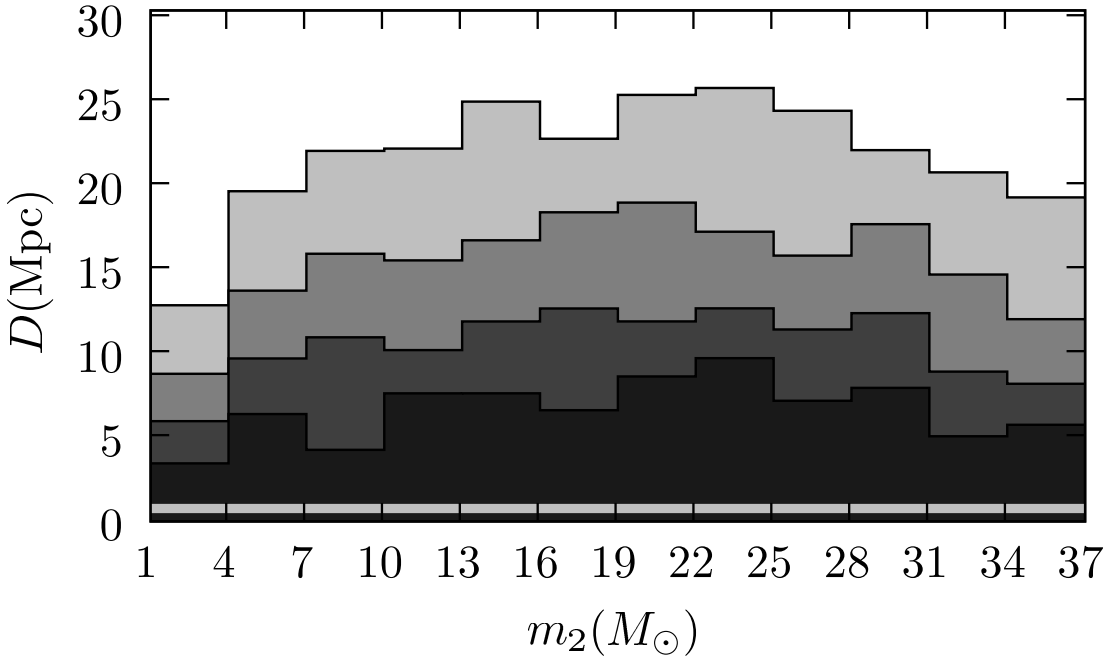

FIG. 3.—Probability as described in eq. (3) computed using injections made only into the 180 s segments immediately before and after the on-source time. The shaded regions represent 90%, 75%, 50%, and 25% exclusion regions, from darkest to lightest, respectively. The distance to M31 is indicated by the horizontal line at $D = 0.77$ Mpc. Both the amplitude calibration uncertainty and Monte Carlo statistics are included in this result; apparent fluctuations as a function of mass are due to Monte Carlo uncertainty.

of whitening, phase calibration, and bandpassing from 40 to 2000 Hz. The cross-correlation is calculated for short time series of equal length taken from the data streams of each detector. For the discretely sampled time series s_1 and s_2, each containing n elements, the cross-correlation, cc, is defined as

$$\mathrm{cc} = \frac{\sum_{i=1}^{n}[s_1(i)-\mu_1][s_2(i)-\mu_2]}{\sqrt{\sum_{j=1}^{n}[s_1(j)-\mu_1]^2}\sqrt{\sum_{k=1}^{n}[s_2(k)-\mu_2]^2}}, \quad (4)$$

where μ_1 and μ_2 are the corresponding means of s_1 and s_2. Possible values of this normalized cross-correlation range from -1 to +1, the minus sign corresponding to anticorrelation and the plus sign to correlation.

The measurement of the cross-correlation statistic proceeded as follows. Both 180 s, on-source time series of H1 and H2 data were divided into time intervals (or cross-correlation windows) of length T_{ccw}. Previous analyses have shown that using two windows, $T_{\mathrm{ccw}} = 25$ and 100 ms, is sufficient to target short-duration signals lasting from $\sim$1 to $\sim$100 ms. The intervals were overlapped by half (i.e., $T_{\mathrm{ccw}}/2$) to avoid missing a signal occurring near a boundary. The cross-correlation value, cc, was calculated for each H1-H2 interval pair and for both T_{ccw} cross-correlation window lengths. The largest cc is the strength measure of the most significant correlated candidate value within the 180 s long on-source segment. To estimate the significance of this loudest event, we use off-source data to measure the cross-correlation distribution of the background noise.

4.2. *Background Estimation and Search Results*

Approximately 3 hr of data symmetrically distributed about the on-source segment were used to study the background. These off-source data were collected from sufficiently close to the on-source time to accurately reflect the statistical properties of the data within the on-source region. The detectors were collecting data continuously during the off- and on-source periods. The off-source data were divided into 180 s long segments, corresponding to the length of the on-source segment. The off-source segments were treated identically to the on-source segment.

The distribution of the largest cc values in the absence of a signal was estimated for each cross-correlation window ($T_{\mathrm{ccw}} = 25$ and 100 ms) by applying the method in § 4.1 for all 180 s long off-source data segments. To increase the off-source distribution statistics, time shifts between the H1 and H2 data streams were also performed. The H1 data stream was shifted by multiples of 180 s relative to H2. Then two 180 s stretches from the two detectors were paired at each shift, making sure that two 180 s time stretches were paired only once. The distribution of cross-correlations obtained with time-shifted data is consistent with what is obtained from unshifted data. For both cross-correlation windows (T_{ccw}), the resulting off-source loudest event cc distribution was used to estimate the probability that background noise alone (i.e., without a gravitational-wave signal) would produce a cc value larger than the largest cross-correlation found in the on-source segment.

Figure 4 shows the cumulative cross-correlation distribution for the $T_{\mathrm{ccw}} = 25$ and 100 ms cases. For the $T_{\mathrm{ccw}} = 25$ ms time window, the largest cross-correlation found in the on-source data was cc = 0.36 (see Fig. 4*a*, *arrow*). The probability of obtaining a cross-correlation value this large from noise alone is 0.58. For the $T_{\mathrm{ccw}} = 100$ ms time window, the largest cross-correlation found in the on-source data was cc = 0.15 (see Fig. 4*b*, *arrow*), and the probability for this cross-correlation value is 0.96. These results are, therefore, consistent with noise. We conclude that no gravitational-wave burst associated with GRB 070201 was detected by the search.

4.3. *Upper Limits on the Amplitude and Energy of Gravitational-Wave Transients Associated with GRB 070201*

Since the analysis of the previous section showed no evidence for a gravitational-wave burst, we set upper limits on the amplitude

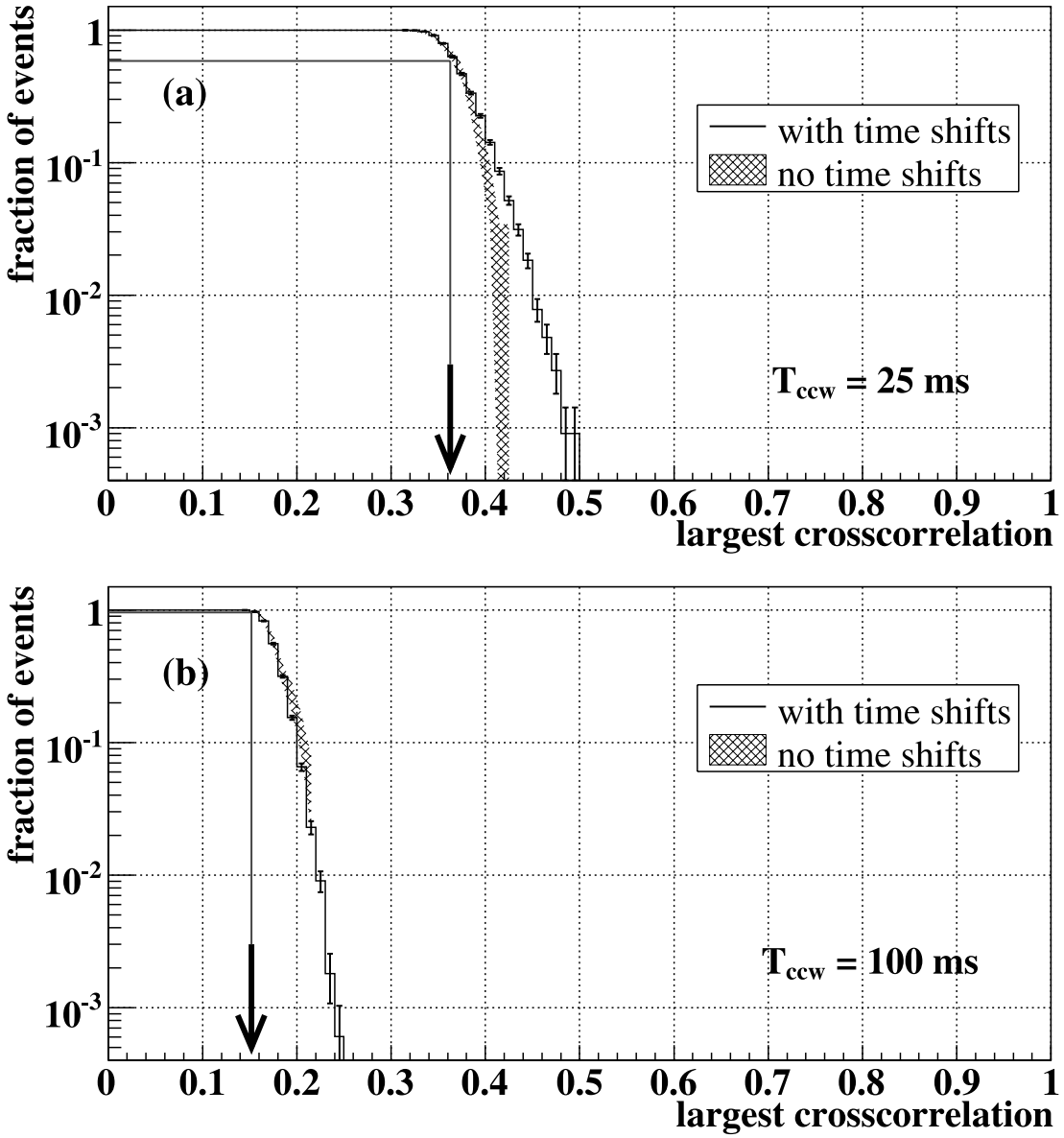

FIG. 4.—Cumulative distribution of measured cross-correlation values for the (*a*) $T_{ccw} = 25$ ms and (*b*) $T_{ccw} = 100$ ms cross-correlation windows. Both distributions with and without time shifts are shown, including the statistical errors. The arrows in both cases point to the largest cross-correlation found in the on-source segment. For the background distributions, 1 minus cumulative distribution is plotted.

and energy of gravitational waves incident on the detectors during GRB 070201. Denote the gravitational-wave signal by $h(t; h_{rss})$, where

$$h_{rss} = \sqrt{\int_{-\infty}^{\infty} \left[|h_+(t)|^2 + |h_\times(t)|^2 \right] dt} \tag{5}$$

is the root-sum-squared amplitude of the gravitational-wave signal. To determine an upper limit, one needs the probability of measuring cc given the presence of a signal with h_{rss},

$$p[\mathrm{cc}|h(t; h_{rss})]. \tag{6}$$

The search targets signals with durations $\lesssim$100 ms. Within this class of signals, the sensitivity of the search has a weak dependence on signal morphology; it depends primarily on the energy and the frequency content of the signal. Therefore, as long as the frequency and duration of the injected test waveforms match the theoretical predictions, we can work with the waveform of our choice. A class of waveforms called *sine-Gaussians* have become the standard benchmark for burst searches and were used to construct the probability distribution given in equation (6). The explicit formulae for $h_+(t)$ and $h_\times(t)$ are

$$h_+(t) = h_0 \sin[2\pi f_0(t - t_0)] \exp\left\{ \frac{-[2\pi f_0(t - t_0)]^2}{2Q^2} \right\}, \tag{7}$$

$$h_\times(t) = h_0 \cos[2\pi f_0(t - t_0)] \exp\left\{ \frac{-[2\pi f_0(t - t_0)]^2}{2Q^2} \right\}, \tag{8}$$

where f_0 is the central frequency, h_0 is the peak amplitude of each polarization, t_0 is the peak time, and Q is a dimensionless constant that represents roughly the number of cycles with which the waveform oscillates with more than half of the peak amplitude. Since the $h_+(t)$ and $h_\times(t)$ waveforms have the same amplitude, these simulated gravitational-wave bursts are circularly polarized.

TABLE 1
90% Amplitude Upper Limits and Corresponding Characteristic Energies from sine-Gaussian Waveform Simulations

SG Central Frequency (Hz)	T_{ccw} (ms)	90% UL on h_{rss} ($Hz^{-1/2}$)	Characteristic E_{GW}^{iso} ($M_\odot c^2$)	Characteristic E_{GW}^{iso} (ergs)
100	25	2.15×10^{-21}	5.8×10^{-4}	1.0×10^{51}
150	25	1.27×10^{-21}	4.6×10^{-4}	8.2×10^{50}
250	25	1.34×10^{-21}	1.4×10^{-3}	2.5×10^{51}
554	25	2.36×10^{-21}	2.1×10^{-2}	3.8×10^{52}
1000	25	4.12×10^{-21}	2.1×10^{-1}	3.8×10^{53}
1850	25	7.56×10^{-21}	2.5	4.5×10^{54}
100	100	1.97×10^{-21}	4.9×10^{-4}	8.8×10^{50}
150	100	1.25×10^{-21}	4.4×10^{-4}	7.9×10^{50}
250	100	1.41×10^{-21}	1.6×10^{-3}	2.9×10^{51}
554	100	2.52×10^{-21}	2.5×10^{-2}	4.5×10^{52}
1000	100	4.51×10^{-21}	2.6×10^{-1}	4.7×10^{53}
1850	100	8.15×10^{-21}	2.9	5.2×10^{54}

Notes.—Assuming 770 kpc as source distance. The h_{rss} limits given in the table already include the calibration and statistical errors (Abbott et al. 2008a).

We provide results for the characteristic case of $Q = 8.9$, as the dependence of the upper limits on Q is very weak. The measurement is carried out as follows. First, we choose a central frequency, f_0, and an h_{rss} value for the injected signal. From these parameters, we calculate $h(t)$ using equations (1), (5), (7), and (8). We then add the calibrated $h(t)$ to the on-source H1 and H2 data, choosing a random starting time within the segments. We then measure the largest value of cross-correlation, cc, generally following the same method described in § 4.1, except that in this case only a shorter interval around the injection is searched. Using the same h_{rss} values, we keep iterating the last two steps of the algorithm (randomizing a starting point and calculating the cc local maximum) until we have enough data points to determine the conditional probability $p(\mathrm{cc}|h_{rss})$. This probability, determined for different h_{rss} values and central frequencies, is then used to set a frequentist upper limit on h_{rss}, given the largest cross-correlation found for the on-source segment in the search (see § 4.1; Abbott et al. 2008a).

The resulting 90% h_{rss} upper limits are given in Table 1 for circularly polarized sine-Gaussians with different central frequencies and $Q = 8.9$. The frequency dependence of the upper limits follows the shape of the detector's frequency-dependent noise spectrum.

The h_{rss} limits given in Table 1 include the calibration and statistical errors. These errors were propagated into the 90% h_{rss} upper limits using the same procedure used in Abbott et al. (2008a). The 1 σ errors considered were (1) calibration response phase error (10°), (2) calibration response amplitude error (10%), and (3) statistical error determined through Monte Carlo simulations (2.1%).

The upper limits on h_{rss} implied by the burst search can be translated into conventional astrophysical units of energy emitted in gravitational waves. The gravitational-wave energy E_{GW} radiated by an *isotropically emitting* source that is dominated by emission at a frequency f_0 is related to the h_{rss} received at distance D, much less than the Hubble distance, by (Riles 2004)

$$E_{GW}^{iso} \approx \frac{\pi^2 c^3}{G} D^2 f_0^2 h_{rss}^2. \quad (9)$$

Based on the sensitivity of this burst search as summarized in Table 1, we estimate that a gravitational-wave burst with characteristic frequency in the most sensitive frequency region of the LIGO detectors ($f \approx 150$ Hz), if GRB 070201 originated in M31 (at 770 kpc), must have emitted less than approximately $4.4\times10^{-4}\ M_\odot c^2$ (7.9×10^{50} ergs) within any 100 ms interval in the on-source window in gravitational waves. In terms of the SGR progenitor hypothesis, our experimental upper limit on E_{GW} is several orders of magnitude larger than the 10^{45} ergs $(D/770\ \mathrm{kpc})^2$ known to be emitted electromagnetically. And while present models for SGR bursts may differ substantially in their mechanisms (de Freitas Pacheco 1998; Ioka 2001; Owen 2005; Horvath 2005), they suggest that no more than 10^{46} ergs is released in the form of gravitational waves. Therefore, the upper limit achievable with the present detectors does not exclude these models of SGRs at the M31 distance.

We also estimate the sensitivity of the (100 ms) burst search to gravitational waves from a compact binary progenitor in M31 (see Fig. 5). We choose as examples a 1.4 $M_\odot$–1.4 $M_\odot$ binary and a 1.4 $M_\odot$–10 $M_\odot$ binary. For each mass pair, we inject approximately 1000 inspiral waveforms consistent with the distance of M31, with random isotropically distributed inclination and polarization, and with coalescence time uniformly distributed through the on-source segment. Since, for these masses, the merger phase is expected to occur at frequencies well above that of maximum LIGO sensitivity, we inject only the inspiral portion. As for the sine-Gaussian simulations, we determine the largest cross-correlation within a small time window around the coalescence time. We also account for possible systematic errors due to the calibration and the uncertainty in the distance to a possible source within M31 and statistical errors from the Monte Carlo procedure. We estimate with 90% confidence that a 1.4 $M_\odot$–1.4 $M_\odot$ binary inspiral in M31 at the time of GRB 070201 would have a probability of at least 0.878 of producing a cross-correlation larger than the loudest on-source event. For 1.4 $M_\odot$–10 $M_\odot$ binaries this probability is at least 0.989. This gives us an independent way to reject the hypothesis of a compact binary progenitor in M31, while not relying on the detailed model of the inspiral signal.

5. DISCUSSION

We analyzed the data from the LIGO H1 and H2 gravitational-wave detectors, looking for signals associated with the electromagnetic event GRB 070201. No plausible gravitational-wave signals were identified. Based on this search, a compact binary progenitor (neutron star + black hole or neutron star systems) of GRB 070201, with masses in the range 1 $M_\odot < m_1 < 3\ M_\odot$ and

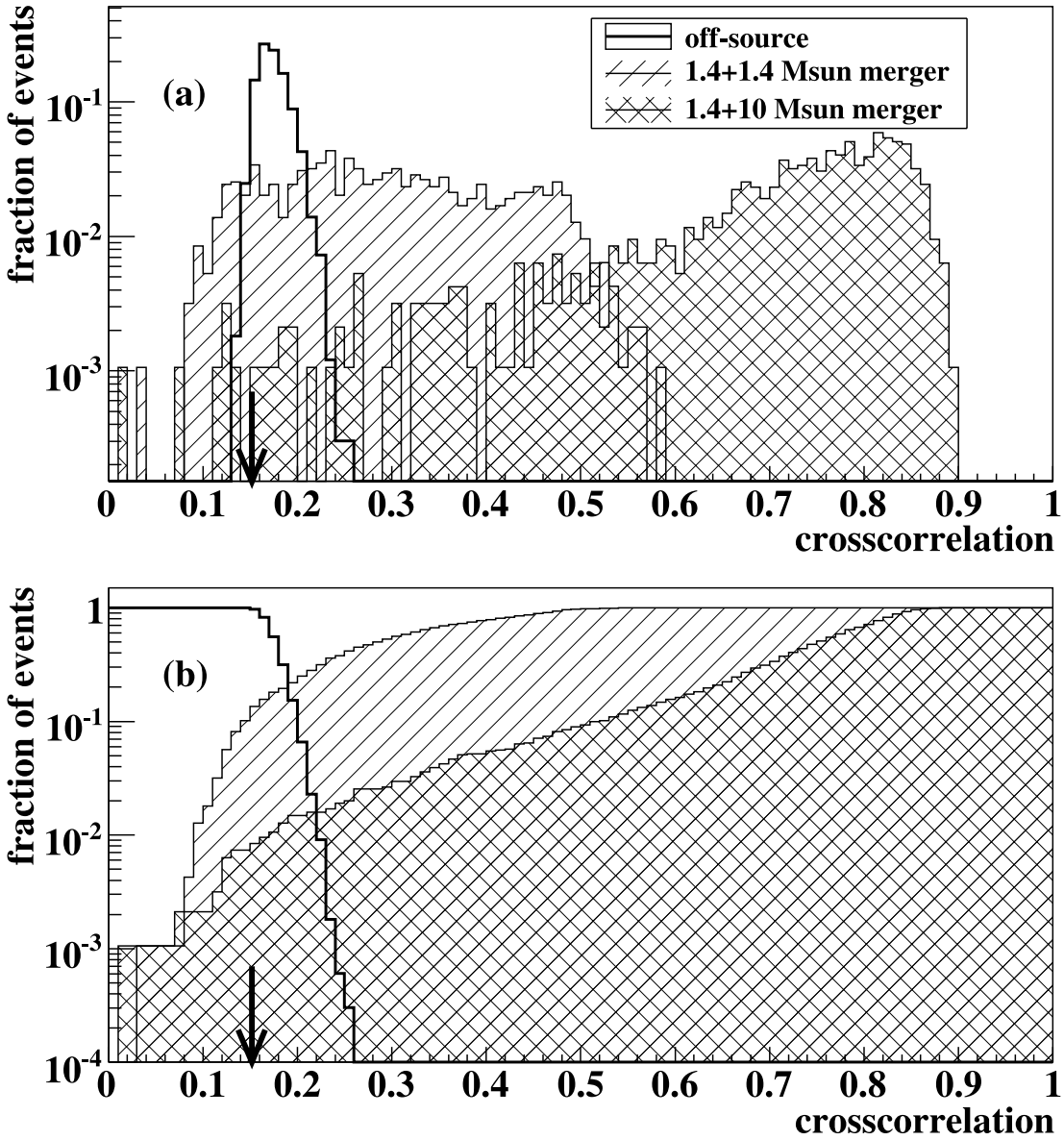

FIG. 5.—Differential (*a*) and cumulative (*b*) distributions of measured cross-correlation values for the $T_{ccw} = 100$ ms cross-correlation window. Distributions for both the 1.4 $M_\odot$–1.4 $M_\odot$ and 1.4 $M_\odot$–10 $M_\odot$ binaries are shown along with the background distribution. The arrows point to the largest cross-correlation found in the on-source segment. In (*b*), 1 minus cumulative distribution of the off-source data is plotted.

1 $M_\odot < m_2 < 40\ M_\odot$, located in M31 is excluded at >99% confidence. If GRB 070201 was caused by a binary neutron star merger not in M31, then we find that distances $D < 3.5$ Mpc to the system are excluded, assuming random inclination, at 90% confidence.

Our model-independent search did not find correlated signatures inconsistent with the noise within the H1 and H2 data streams that could be related to GRB 070201. Based on the sensitivity of our search and assuming isotropic gravitational-wave emission of the progenitor, an upper limit on the power emitted in gravitational waves by GRB 070201 was determined. A gravitational wave with characteristic frequency within the most sensitive range of the LIGO detectors ($f \approx 150$ Hz) most probably emitted less than $E_{GW} < 7.9 \times 10^{50}$ ergs within any 100 ms long time interval inside the on-source region if the source is in M31. This limit on radiated power is comparable to the emitted power of some GRBs. However, it is significantly higher than the associated electromagnetic emission of this particular GRB. Therefore, the transient search only constrains the binary inspiral models for a short, hard GRB in M31 and does not impose new limitations on magnetar-driven (SGR-type) burst models.

As gravitational-wave observations continue and the sensitivity of the instruments improves, we look forward to the astrophysical insights that combined electromagnetic and gravitational observing campaigns can bring.

We are indebted to the observers of the electromagnetic event, GCN and IPN, for providing us with valuable data and real-time information. We are grateful to Neil Gehrels of NASA/GSFC for his help in reviewing the article. The authors gratefully acknowledge the support of the United States National Science Foundation for the construction and operation of the LIGO Laboratory and the Science and Technology Facilities Council of the United Kingdom, the Max Planck Society, and the State of Niedersachsen/Germany for support of the construction and operation of the GEO-600 detector. The authors also gratefully acknowledge the support of

the research by these agencies and by the Australian Research Council, the Council of Scientific and Industrial Research of India, the Istituto Nazionale di Fisica Nucleare of Italy, the Spanish Ministerio de Educación y Ciencia, the Conselleria d'Economia, Hisenda i Innovació of the Govern de les Illes Balears, the Scottish Funding Council, the Scottish Universities Physics Alliance, the National Aeronautics and Space Administration, the Carnegie Trust, the Leverhulme Trust, the David and Lucile Packard Foundation, the Research Corporation, and the Alfred P. Sloan Foundation. We are grateful to the *GALEX* collaboration for providing the UV image of M31, the SDSS project for providing the optical image of M31, and Google Sky for accelerating the error box position verification. This paper was assigned LIGO Document No. LIGO-P070081-B.

REFERENCES

Abbott, B., et al. 2004, Nucl. Instrum. Methods Phys. Res. A, 517, 154
———. 2005a, Phys. Rev. D, 72, 042002
———. 2005b, Phys. Rev. D, 72, 082001
———. 2005c, Phys. Rev. D, 72, 082002
———. 2006a, Classical Quantum Gravity, 23, S29
———. 2006b, Phys. Rev. D, 73, 062001
———. 2008a, Phys. Rev. D, 77, 062004
———. 2008b, Phys. Rev. D, 77, 062002
Acernese, F., et al. 2006, Classical Quantum Gravity, 23, S635
Adelman-McCarthy, J. K., et al. 2006, ApJS, 162, 38
Allen, B. 2005, Phys. Rev. D, 71, 062001
Allen, B. A., Anderson, W. G., Brady, P. R., Brown, D. A., & Creighton, J. D. E. 2005, preprint (gr-qc/0509116)
Berger, E. 2007, ApJ, 670, 1254
Blanchet, L. 2006, Living Rev. Relativ., 9, 4
Bloom, J. S., et al. 2007, ApJ, 654, 878
Burrows, D. N., et al. 2006, ApJ, 653, 468
Campana, S., et al. 2006, Nature, 442, 1008
Chapman, R., Priddey, R. S., & Tanvir, N. R. 2008, in AIP Conf. Proc. 983, 40 Years of Pulsars: Millisecond Pulsars, Magnetars and More, ed. C. G. Bassa (New York: AIP), 304
Cook, G. B., Shapiro, S. L., & Teukolsky, S. A. 1994, ApJ, 424, 823
de Freitas Pacheco, J. A. 1998, A&A, 336, 397
Finn, L. S., Krishnan, B., & Sutton, P. J. 2004, ApJ, 607, 384
Freedman, W. L., et al. 2001, ApJ, 553, 47
Frontera, F., et al. 2000, ApJS, 127, 59
Galama, T. J., et al. 1998, Nature, 395, 670
Gehrels, N., et al. 2004, ApJ, 611, 1005
———. 2006, Nature, 444, 1044
Golenetskii, S., Aptekar, R., Mazets, E., Pal'shin, V., Frederiks, D., & Cline, T. 2007a, GRB Circ., 6094, 1
Golenetskii, S., et al. 2007b, GRB Circ., 6088, 1
Grandclement, P., Kalogera, V., & Vecchio, A. 2003, Phys. Rev. D, 67, 042003
Grupe, D., Burrows, D. N., Patel, S. K., Kouveliotou, C., Zhang, B., Mészáros, P., Wijers, R. A. M., & Gehrels, N. 2006, ApJ, 653, 462
Hjorth, J., et al. 2003, Nature, 423, 847
Horvath, J. E. 2005, Mod. Phys. Lett. A, 20, 2799
Hurley, K., et al. 2005, Nature, 434, 1098
———. 2007, GRB Circ., 6103, 1
Ioka, K. 2001, MNRAS, 327, 639
Jakobsson, P., et al. 2006, A&A, 447, 897
Kawai, N., et al. 2006, Nature, 440, 184
Klebesadel, R. W., Strong, I. B., & Olson, R. A. 1973, ApJ, 182, L85
Kochanek, C. S., & Piran, T. 1993, ApJ, 417, L17
Kouveliotou, C., Meegan, C. A., Fishman, G. J., Bhat, N. P., Briggs, M. S., Koshut, T. M., Paciesas, W. S., & Pendleton, G. N. 1993, ApJ, 413, L101
Malesani, D., et al. 2004, ApJ, 609, L5
Mazets, E. P., & Golenetskii, S. V. 1981, Ap&SS, 75, 47
Mazets, E., et al. 2008, ApJ, 680, 545
McClintock, J. E., et al. 2006, ApJ, 652, 518
Meegan, C. A., Fishman, G. J., Wilson, R. B., Horack, J. M., Brock, M. N., Paciesas, W. S., Pendleton, G. N., & Kouveliotou, C. 1992, Nature, 355, 143
Mészáros, P. 2002, ARA&A, 40, 137
Nakar, E. 2007, Phys. Rep., 442, 166
Nakar, E., Gal-Yam, A., Piran, T., & Fox, D. B. 2006, ApJ, 640, 849
O'Shaughnessy, R., Kaplan, J., Kalogera, V., & Belczynski, K. 2005, ApJ, 632, 1035
Owen, B. J. 2005, Phys. Rev. Lett., 95, 211101
Paciesas, W. S., et al. 1999, ApJS, 122, 465
Palmer, D. M., et al. 2005, Nature, 434, 1107
Pal'shin, V. 2007, GRB Circ., 6098, 1
Perley, D. A., & Bloom, J. S. 2007, GRB Circ., 6091, 1
Piran, T. 2005, Rev. Mod. Phys., 76, 1143
Rantsiou, E., Kobayashi, S., Laguna, P., & Rasio, F. 2008, ApJ, in press (astro-ph/0703599)
Riles, K. 2004, Notes on Relating Sine-Gaussian Waveforms to Astrophysical Source Strengths (LIGO note T040055-00-Z; Pasadena: Caltech), http://www.ligo.caltech.edu/docs/T/T040055-00.pdf
Rodriguez, A. 2007, M.S. thesis, Louisiana State Univ.
Soderberg, A. M., et al. 2006, ApJ, 650, 261
Thilker, D. A., et al. 2005, ApJ, 619, L67
Thorne, K. S. 1974, ApJ, 191, 507
Vallisneri, M. 2000, Phys. Rev. Lett., 84, 3519
Wainstein, L. A., & Zubakov, V. D. 1962, Extraction of Signals from Noise (Englewood Cliffs: Prentice-Hall)
Watson, D., Reeves, J. N., Hjorth, J., Fynbo, J. P. U., Jakobsson, P., Pedersen, K., Sollerman, J., Castro Cerón, J. M., McBreen, S., & Foley, S. 2006, ApJ, 637, L69
Willke, B., et al. 2002, Classical and Quantum Gravity, 19, 1377
Woosley, S. E., & Bloom, J. S. 2006, ARA&A, 44, 507